additional observations on the question of bond order/bond length, so far as manganese complexes are concerned. For example, when one compares the shortest[51c] Mn–Mn distance for a compound with BO = 0 with the longest[48b] distance for BO = 1, the difference is only 0.021 Å. A larger (0.109 Å) deviation is observed when the shortest[48a] BO = 1 distance is compared with that recently reported for $Cp_2Mn_2[\mu\text{-NN-}(SeMe_3)_2]_2$[51a] (BO = 2). By comparison, the overall range of Mn–Mn distances for compounds with EAN BO = 1 is 0.712 Å. This is the broadest range in single-bond distances that we know of, and it indicates (at least to us) a need for caution in using simple rules (such as the EAN rule) to explain metal–metal distances.

Registry No. 1, 57603-42-6.

Supplementary Material Available: A listing of observed and calculated structure factors for the Mn dimer (18 pages). Ordering information is given on any current masthead page.

Contribution from the Department of Chemistry,
University of Colorado, Boulder, Colorado 80309

Molybdenum Complexes Containing Catecholate Ligands. Structural Studies on Complexes of the Pentaoxobis(quinone)dimolybdate(*n*−) (*n* = 0, 1, 2) Redox Series

CORTLANDT G. PIERPONT* and ROBERT M. BUCHANAN

Received May 22, 1981

Members of the $Mo_2O_5(quinone)_2^{n-}$ (*n* = 0, 1, 2) series have been synthesized. The neutral complex prepared with 9,10-phenanthrenequinone, $Mo_2O_5(9,10\text{-phenSQ})_2$, has been characterized in a previous structural study. The dianion containing 3,5-di-*tert*-butylcatechol has been prepared and reported previously. We now report the results of a structural investigation on this dianion, obtained as the tetra-*n*-butylammonium salt. Structural features of the $Mo_2O_5^{2+}$ region of the complex closely resemble those of the neutral molecule. This result together with the features of the quinone ligands in both structures shows that the charge difference is contained entirely within the quinones. The monoanion formulated as the mixed-ligand complex $Mo_2O_5(3,5\text{-DBCat})(3,5\text{-DBSQ})^-$ has been prepared by Ag^+ oxidation of the dianion. The EPR spectrum of this $S = {}^1/_2$ complex is virtually identical with that of a free semiquinone, indicating that spin density is localized on only one of the two quinone ligands at room temperature. Oxygen atom transfer reactions involving molybdenum–catecholate complexes are also discussed.

Introduction

Among the earliest reports of transition-metal complexes prepared with catecholate ligands are a series of compounds prepared with molybdate ion.[1–4] These compounds and the solution chemistry of Mo(VI)–catechol systems have become of particular importance as a photometric analytical method for the determination of molybdenum.[5,6] In neutral solution a red-orange complex with a Mo:catechol ratio of 1:2 is formed, while at pH values below 2 a 1:1 complex is observed.[7] Atovmyan has characterized products of early synthetic reactions crystallographically, and found them to contain the $MoO_2(Cat)_2^{2-}$ and $Mo_2O_5(Cat)_2^{2-}$ ions.[8,9] These reports were the first structural studies carried out on transition-metal complexes containing catecholate ligands. More recently kinetic studies have been carried out on the molybdate–catechol system[10] and the redox chemistry of molybdenum–catecholate complexes has been investigated in detail.[11–13]

Table I. Crystallographic Data for $(n\text{-}Bu_4N)_2[Mo_2O_5(3,5\text{-DBCat})_2]$

fw	1197.6	*Z*	4
space group	$P2_12_12_1$	μ, cm^{-1}	4.41
	(D_2^4,	Mo Kα radiation	λ = 0.710 69 Å
	No. 19)	scan rate, deg min^{-1}	4
a, Å	14.293 (2)	max 2θ, deg	50
b, Å	17.515 (2)	scan range, deg	±0.7
c, Å	28.218 (5)	data collected	7035
V, $Å^3$	7064.3	unique data, $I > 3\sigma(I)$	3494
d_{calcd}, g cm^{-3}	1.126		
d_{exptl}, g cm^{-3}	1.13		

Research carried out in our laboratory, which has been directed at investigation of the coordination chemistry of quinone ligands, has also included work with molybdenum. Procedures used to synthesize complexes of molybdenum in aprotic media have involved oxidation of Mo(0) in $Mo(CO)_6$ by the *o*-benzoquinone form of the ligand. Results obtained by this procedure have shown a surprising ligand dependence (1).[14–16] Each product has been characterized structurally;

---

(1) Weinland, R. F.; Gaisser, F. *Z. Anorg. Allg. Chem.* **1919**, *108*, 231.
(2) Weinland, R. F.; Huthmann, P. *Arch. Pharm. Ber. Dtsch. Pharm. Ges.* **1924**, *262*, 329.
(3) Weinland, R. F.; Babel, A. *Z. Anorg. Allg. Chem.* **1925**, *150*, 177.
(4) Fernandes, H. *Gazz. Chim. Ital.* **1925**, *55*, 424.
(5) Seifter, S.; Novic, B. *Anal. Chem.* **1951**, *23*, 188.
(6) Soni, R.; Bartusek, M. *J. Inorg. Nucl. Chem.* **1971**, *33*, 2557.
(7) Haight, G. P., Jr.; Pargamian, V. *Anal. Chem.* **1960**, *32*, 642.
(8) Atovmyan, L. O.; Sokolova, Y. A.; Tkachev, V. V. *Dokl. Akad. Nauk SSSR* **1970**, *195*, 1355.
(9) Atovmyan, L. O.; Tkachev, V. V.; Shiskova, T. G. *Dokl. Akad. Nauk SSR* **1972**, *205*, 609.
(10) Kustin, K.; Kiu, S.-T. *J. Am. Chem. Soc.* **1973**, *95*, 2487.
(11) Wilshire, S. P.; Leon, L.; Bosserman, P.; Sawyer, D. T.; Buchanan, R. M.; Pierpont, C. G. *Chem. Uses Molybdenum, Proc. Int. Conf., 3rd* **1979**, 264.
(12) Wilshire, J. P.; Leon, L.; Bosserman, P.; Sawyer, D. T. *J. Am. Chem. Soc.* **1979**, *101*, 3379.
(13) Wilshire, J. P.; Leon, L.; Bosserman, P.; Sawyer, D. T. "Molybdenum Chemistry of Biological Significance"; Newton, W. E., Otsuka, S., Eds.; Plenum Press: New York, 1980; p 327.
(14) Pierpont, C. G.; Downs, H. H. *J. Am. Chem. Soc.* **1975**, *97*, 2123.
(15) Pierpont, C. G.; Buchanan, R. M. *J. Am. Chem. Soc.* **1975**, *97*, 6450.

0020-1669/82/1321-0652$01.25/0

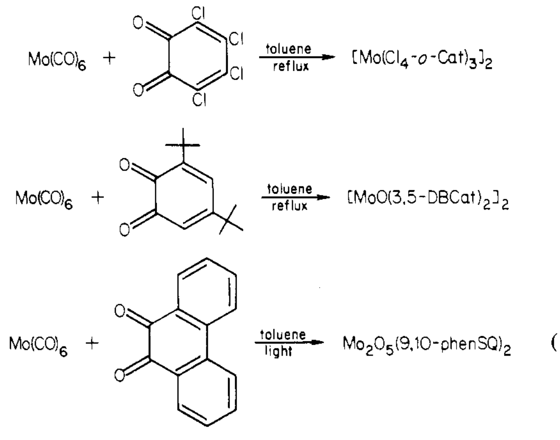

(1)

further research is being focused on the interrelationship of these compounds. The product obtained with 3,5-di-*tert*-butylbenzoquinone, $[MoO(3,5\text{-}DBCat)_2]_2$ has also been prepared by Sawyer and co-workers[12] by treating $MoO_2(acac)_2$ with the catecholate form of the ligand. The dimeric structure found for the complex in the solid state persists in solution in the absence of additional ligating agents. In a coordinating solvent or with additional ligand a monomeric species *trans*-$MoO(L)(3,5\text{-}DBCat)_2$ is formed. The subject of this report is the product obtained by treating $[MoO(3,5\text{-}DBCat)_2]_2$ with strong base in an aprotic solvent medium.[11]

Experimental Section

A crystalline sample of an orange compound found subsequently in our study to be $[(n\text{-}Bu)_4N]_2[Mo_2O_5(3,5\text{-}DBCat)_2]$ was provided by Professor Donald Sawyer of the University of California, Riverside. Preparative procedures have been described previously.[11]

Structure Determination

A crystal of $[(n\text{-}Bu)_4N]_2[Mo_2O_5(3,5\text{-}DBCat)_2]$ was mounted and centered on a Syntex P$\bar{1}$ automated diffractometer. Preliminary photographs taken on this crystal indicated orthorhombic symmetry; systematic absences were consistent with space group $P2_12_12_1$. The centered settings of 15 reflections were used to calculate the cell constants given in Table I. Standard reflections monitored during data collection showed no significant deviations in intensity. Data were processed in the usual way, and the structure was solved with use of standard heavy-atom procedures. Rotational disorder was found for one ligand *tert*-butyl group, C(12)–C(15) in Table II. The end carbon atom of one *n*-butyl chain, C(44), was poorly defined on the Fourier map. Off-diagonal anisotropic thermal parameter terms were fixed at zero for this atom. Final refinement of the structure converged with $R_F = 0.076$ and $R_{wF} = 0.082$ for 3494 reflections with $F_o^2 > 3\sigma(F_o^2)$. The error in an observation of unit weight was 2.03. Computer programs, calculational procedures, and sources of scattering factors have been noted previously.[17] Final positional and thermal parameters for all atoms are given in Table II.

Description of the $Mo_2O_5(3,5\text{-}DBCat)_2^{2-}$ Anion

The $Mo_2O_5(3,5\text{-}DBCat)_2^{2-}$ anion has approximate twofold symmetry with catecholate ligands chelated to one metal ion and bridged to the second through one oxygen. A view of the complex is shown in Figure 1. Bond distances and selected bond angles are given in Table III. Features of the $Mo_2O_5(3,5\text{-}DBCat)_2^{2-}$ anion resemble the neutral 9,10-phenanthrenesemiquinone complex, $Mo_2O_5(9,10\text{-}phenSQ)_2$ shown in Figure 2.[15] The Mo_2O_5 fragments of both molecules are nearly identical. Molybdenum–oxygen lengths to the terminal oxo ligands are nearly identical and are in the 1.68-Å range associated with *cis*-dioxomolybdenum(VI) species. The Mo-O(1) lengths in the anion average to 1.919 (10) Å, slightly longer than the 1.898-Å value of Mo_2O_5 $(9,10\text{-}phenSQ)_2$. Similar values were reported by Atovmyan for $Mo_2O_5(Cat)_2^{2-}$.

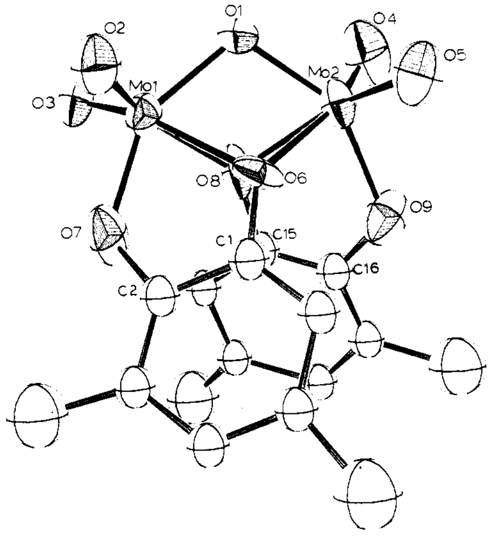

Figure 1. View of the $Mo_2O_5(3,5\text{-}DBCat)_2^{2-}$ anion. Methyl carbon atoms of the ligand *tert*-butyl groups have been omitted.

The nonbonding Mo–Mo separation in the present complex is 3.132 (4) Å compared with 3.160 (2) Å for $Mo_2O_5(9,10\text{-}phenSQ)_2$ and 3.13 (1) Å for $Mo_2O_5(Cat)_2^{2-}$. The two-electron charge difference between $Mo_2O_5(9,10\text{-}phenSQ)_2$ and $Mo_2O_5(3,5\text{-}DBCat)_2^{2-}$ appears contained entirely within the quinone ligands with no significant effect on the $Mo_2O_5^{2+}$ portion of the complex.

Catecholate oxygen atoms of $Mo_2O_5(3,5\text{-}DBCat)_2^{2-}$ appear to be slightly better donors to the Mo(VI) center than semiquinone oxygens of $Mo_2O_5(9,10\text{-}phenSQ)_2$. The Mo(1)–O(7) and Mo(2)–O(9) lengths of the anion average 1.977 (10) Å compared with a value of 2.041 (4) Å for similar lengths of the neutral molecule. The bridging ligand oxygen atoms of the anion have Mo–O lengths of 2.156 (9) Å within the chelate ring and 2.385 (10) Å to outer metal atoms. Related values were found to be approximately 0.1 Å longer for $Mo_2O_5(9,10\text{-}phenSQ)_2$. For the Co(III) complex Co(3,5-DBCat)(3,5-DBSQ)(bpy) there was no significant difference between catecholate and semiquinone Co–O lengths.[18] Structural features of the catecholate ligands are standard with C–O lengths averaging to 1.37 (2) Å and ring carbon–carbon lengths consistent with an aromatic structure.[19]

Despite the presence of paramagnetic semiquinone ligands, the $Mo_2O_5(9,10\text{-}phenSQ)_2$ molecule is diamagnetic. Close proximity of the π systems of the two ligands (Figure 2) appears to result in direct spin coupling between semiquinones at the $Mo_2O_5^{2+}$ unit. Structural features that support this are the close interplanar and interatomic contacts between ligands and the dihedral angle between ligand planes, 19.3°. With two additional ligand electrons a repulsive interaction might be expected. In fact, the dihedral angle between ligand planes for the dianion is 50.0 (4)°. End views of the two molecules given in Figure 3 show the difference in ligand coplanarity for the two complexes. The increase in dihedral angle need not be solely related to the change in electronic structure. Steric interactions between *tert*-butyl groups of adjacent ligands could also contribute. It would be of interest to perform similar calculations for $Mo_2O_5(Cat)_2^{2-}$; however, atomic parameters are not available for this structure determination. Shortest interligand separations for $Mo_2O_5(9,10\text{-}phenSQ)_2$ occur between bridging quinone oxygen atoms and carbon atoms at the upper portion of the quinone ring. Oxygen–oxygen separations, corresponding to the O(6)–O(8) separation in Figure

---

(16) Buchanan, R. M.; Pierpont, C. G. *Inorg. Chem.* **1979**, *18*, 1616.

(17) Pierpont, C. G. *Inorg. Chem.* **1977**, *16*, 2970.

(18) Buchanan, R. M.; Pierpont, C. G. *J. Am. Chem. Soc.* **1980**, *102*, 4951.

(19) Pierpont, C. G.; Buchanan, R. M. *Coord. Chem. Rev.*, in press.

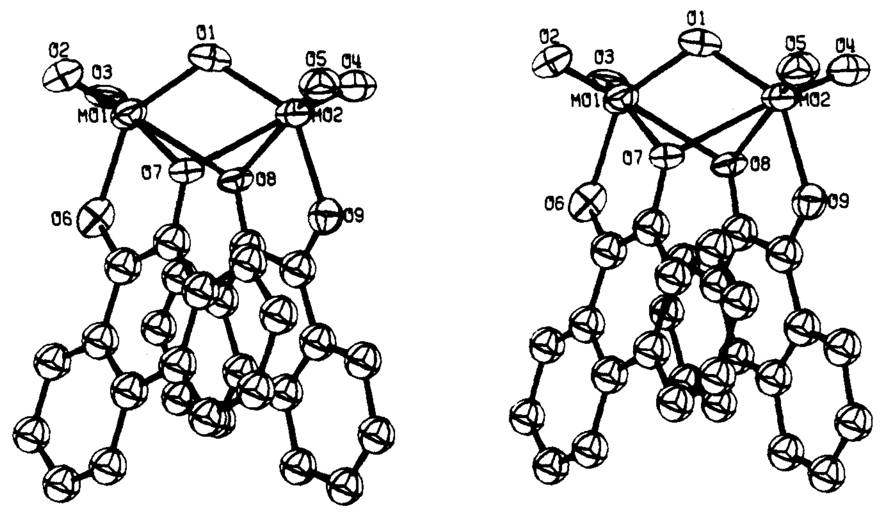

Figure 2. Stereoview of the $Mo_2O_5(9,10\text{-phenSQ})_2$ complex molecule.

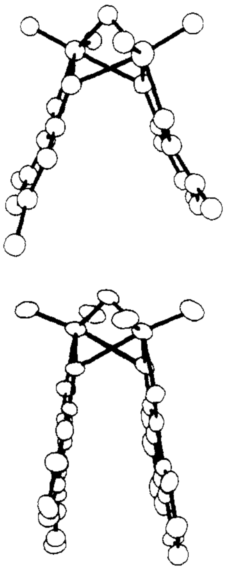

Figure 3. View showing the ligand-pairing interaction for the $Mo_2O_5(3,5\text{-DBCat})_2^{2-}$ anion (top) and the neutral $Mo_2O_5(9,10\text{-phenSQ})_2$ molecule (bottom). The dihedral angle between ligand planes for the anion is 50.0 (4)°; for the neutral molecule the angle is 19.3°.

1, are nearly identical for both structures: 2.66 (1) Å for the dianion and 2.648 (2) Å for the neutral molecule. This is a normal separation for oxygen donors of a MoO_6 octahedron. Carbon–carbon separations for atoms corresponding to C(1), C(2), C(15), and C(16) in Figure 1 are 2.76–2.77 Å for $Mo_2O_5(9,10\text{-phenSQ})_2$ but are nearly 1 Å longer for the dianion with values ranging from 3.52 (2) to 3.81 (2) Å. This is consistent with the increased dihedral angle and a repulsive interaction between ligand π systems.

Properties of the $Mo_2O_5(\text{quinone})_2^{n-}$ ($n = 0, 1, 2$) Series

In theory a three-membered redox series should exist for the $Mo_2O_5(\text{quinone})_2^{n-}$ complexes with members of the series related by stepwise reduction of the quinone ligands from semiquinone to catecholate. Structural studies on both the neutral and dianionic complexes show that the major structural change that occurs upon reduction is distortion of the parallel planes of the quinone ligands. Electrochemical studies carried out by Sawyer on $Mo_2O_5(3,5\text{-DBCat})_2^{2-}$ seem to indicate reversible one-electron oxidation to the monoanion but that full oxidation to a neutral complex similar to $Mo_2O_5(9,10\text{-phenSQ})_2$ leads to an unstable species, which dissociates in solution. The monoanion is of interest due to the electronic dissimilarity of the quinone ligands. On the assumption that the $Mo_2O_5^{2+}$ portion of the molecule remains unchanged, one of the quinone ligands is bonded as a catechol and the other as a semiquinone, $Mo_2O_5(3,5\text{-DBCat})(3,5\text{-DBSQ})^-$. This opens the possibility for interligand electron transfer, possibly of the type observed for Co(3,5-DBCat)(3,5-DBSQ)(bpy).[18] The mechanism could involve the Mo_2O_5 region of the complex or could result from direct electron transfer between ligands through the interstitial region shown in Figure 3. EPR is a convenient method of analysis due to the appearance of ligand hyperfine. 3,5-Di-*tert*-butylsemiquinone shows strong hyperfine coupling to the ring proton at the 4-position and weaker coupling to the *tert*-butyl protons at the 5-carbon atom.[19] A solution of $Mo_2O_5(3,5\text{-DBSQ})(3,5\text{-DBCat})^-$ was prepared by adding slightly less than 1 equiv of Ag^+ to a dichloromethane solution of $Mo_2O_5(3,5\text{-DBCat})_2^{2-}$ (eq 2). The solution became

Scheme I

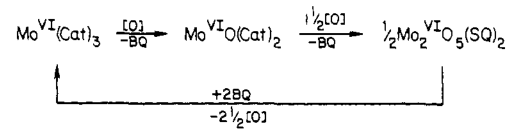

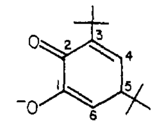

3,5-DBSQ

$$Mo_2O_5(3,5\text{-DBCat})_2^{2-} \xrightarrow[CH_2Cl_2]{Ag^+} Mo_2O_5(3,5\text{-DBCat})(3,5\text{-DBSQ})^- \quad (2)$$

dark brown, and silver metal precipitated as the monoanion formed. The EPR spectrum of the oxidation product was virtually identical with the spectrum of the uncomplexed semiquinone. It showed coupling to a single ring proton with a value of 3.5 G and coupling to a single *tert*-butyl group with a value of 0.3 G. This result is consistent either with complex dissociation to form free semiquinone or with a localized semiquinone–catecholate electronic structure for the complex on the EPR time scale. In the absence of additional hyperfine interactions the EPR spectra of coordinated semiquinones are identical with uncomplexed semiquinones.[19] Sawyer has reported that the dianion can be regenerated from the monoanion by electrolysis. If the monoanion was subject to ligand dissociation, it would likely occur under conditions of the elec-

Table II. Positional and Thermal Parameters for the Atoms of $(n\text{-}Bu_4N)_2[Mo_2O_5(3,5\text{-}DBCat)_2]$

atom	x	y	z	B_{11}[a]	B_{22}	B_{33}	B_{12}	B_{13}	B_{23}
Mo(1)	0.31639 (8)	0.05080 (7)	0.02659 (5)	3.8 (1)	2.7 (1)	4.9 (1)	−0.5 (1)	0.1 (1)	0.7 (1)
Mo(2)	0.13806 (8)	−0.05284 (7)	0.02220 (4)	3.7 (1)	2.7 (1)	3.8 (1)	−0.3 (1)	0.1 (1)	−0.3 (1)
O(1)	0.2315 (7)	−0.0012 (5)	−0.0149 (3)	5.4 (3)	3.8 (5)	2.8 (5)	0.0 (4)	0.2 (5)	0.8 (4)
O(2)	0.4192 (8)	0.0251 (5)	0.0008 (4)	6.4 (3)	4.3 (6)	8.4 (6)	−1.2 (4)	0.2 (5)	0.8 (4)
O(3)	0.3025 (7)	0.1454 (6)	0.0139 (4)	5.2 (3)	4.9 (6)	7.3 (6)	−0.4 (5)	0.0 (5)	−0.3 (5)
O(4)	0.0428 (7)	−0.0293 (5)	−0.0090 (3)	5.8 (4)	4.2 (6)	6.7 (6)	−1.2 (6)	0.0 (5)	−0.9 (4)
O(5)	0.1513 (6)	−0.1481 (5)	0.0125 (3)	3.2 (3)	4.2 (6)	5.9 (7)	−1.1 (5)	−0.5 (5)	−0.5 (4)
O(6)	0.2872 (5)	−0.0570 (5)	0.0611 (3)	3.3 (3)	2.9 (5)	6.4 (6)	−0.3 (5)	−0.5 (4)	0.0 (3)
O(7)	0.3587 (7)	0.0659 (5)	0.0927 (3)	5.9 (4)	3.6 (5)	6.2 (6)	0.0 (5)	−1.6 (4)	0.4 (3)
C(1)	0.3213 (9)	−0.0627 (10)	0.1072 (4)	3.4 (10)	5.1 (10)	3.3 (10)	−0.2 (8)	−1.1 (8)	−1.0 (8)
C(2)	0.3590 (12)	0.0036 (7)	0.1238 (5)	7.6 (12)	1.6 (9)	4.9 (10)	1.1 (9)	−1.4 (8)	−0.6 (8)
C(3)	0.4044 (12)	0.0063 (9)	0.1674 (5)	6.0 (12)	4.7 (10)	4.4 (10)	0.9 (9)	−1.5 (8)	−1.6 (8)
C(4)	0.3991 (12)	−0.0574 (12)	0.1929 (6)	5.9 (11)	7.4 (12)	6.9 (10)	1.6 (9)	−1.9 (8)	1.9 (8)
C(5)	0.3552 (12)	−0.1275 (9)	0.1777 (5)	6.3 (11)	5.1 (10)	4.0 (10)	1.5 (9)	−0.6 (8)	1.0 (8)
C(6)	0.3149 (12)	−0.1277 (8)	0.1332 (5)	7.1 (11)	3.0 (8)	4.6 (10)	1.2 (8)	1.0 (8)	0.7 (8)
C(7)	0.4522 (15)	0.0811 (13)	0.1844 (7)	8.1 (16)	11.6 (20)	8.2 (13)	1.3 (14)	−3.7 (13)	−4.7 (14)
C(8)	0.3775 (17)	0.1467 (10)	0.1920 (7)	15.9 (22)	3.4 (10)	8.2 (13)	2.0 (16)	−2.4 (14)	−2.7 (12)
C(9)	0.5303 (15)	0.1053 (12)	0.1512 (7)	7.9 (15)	10.2 (16)	8.9 (16)	−3.6 (16)	−1.9 (8)	−2.7 (12)
C(10)	0.4997 (18)	0.0637 (13)	0.2354 (7)	14.8 (21)	7.9 (12)	9.6 (17)	0.6 (10)	−6.7 (14)	−2.0 (10)
C(11)	0.3654 (16)	−0.2019 (12)	0.2063 (7)	9.9 (16)	8.5 (15)	6.5 (18)	−2.5 (12)	−4.1 (11)	4.2 (10)
C(12A)[b]	0.394 (4)	−0.2680 (21)	0.1737 (13)	16.5 (24)	3.5 (10)	5.5 (10)	4.4 (18)	−2.2 (10)	−0.2 (12)
C(13A)	0.269 (5)	−0.2032 (23)	0.2311 (17)	25.3 (29)	6.3 (13)	15.2 (18)	−6.9 (21)	−3.7 (12)	0.0 (14)
C(14A)	0.430 (3)	−0.1923 (17)	0.2509 (13)	24.0 (28)	4.0 (10)	12.8 (16)	4.6 (18)	7.4 (16)	3.6 (12)
C(12B)	0.299 (4)	−0.2586 (22)	0.1828 (24)	17.6 (25)	3.0 (10)	6.0 (10)	4.0 (17)	−2.5 (11)	−2.4 (12)
C(13B)	0.356 (4)	−0.1794 (22)	0.2615 (20)	22.0 (30)	7.0 (14)	18.2 (18)	−6.0 (20)	−5.2 (15)	0.0 (15)
C(14B)	0.461 (5)	−0.2091 (21)	0.2146 (23)	30.0 (29)	4.5 (12)	13.7 (19)	4.7 (18)	−1.2 (10)	0.2 (10)
O(8)	0.1616 (5)	0.0547 (5)	0.0568 (2)	4.6 (3)	2.4 (6)	3.2 (6)	0.0 (5)	0.6 (4)	0.8 (3)
O(9)	0.0816 (7)	−0.0662 (5)	0.0855 (3)	6.2 (3)	1.9 (6)	6.4 (6)	−0.8 (5)	2.1 (4)	−0.6 (3)
C(15)	0.1246 (9)	0.0581 (9)	0.1001 (4)	4.6 (10)	2.5 (9)	4.2 (10)	−0.5 (8)	−0.6 (8)	0.9 (8)
C(16)	0.0769 (11)	−0.0050 (8)	0.1151 (5)	5.0 (10)	2.6 (9)	5.7 (10)	1.2 (9)	1.7 (8)	1.0 (8)
C(17)	0.0290 (12)	−0.0062 (9)	0.1563 (5)	5.6 (11)	4.1 (8)	4.4 (10)	0.1 (9)	1.6 (8)	0.6 (8)
C(18)	0.0308 (13)	0.0631 (9)	0.1843 (5)	11.0 (13)	3.8 (10)	3.1 (6)	1.0 (10)	2.4 (8)	−0.3 (8)
C(19)	0.0790 (12)	0.1272 (9)	0.1692 (5)	7.9 (13)	3.9 (10)	3.6 (10)	−0.1 (9)	0.6 (10)	−1.7 (8)
C(20)	0.1262 (11)	0.1264 (8)	0.1275 (5)	4.8 (11)	3.7 (10)	4.5 (10)	0.8 (7)	−0.5 (8)	−1.4 (8)
C(21)	−0.0279 (15)	−0.0745 (12)	0.1717 (6)	9.1 (16)	8.9 (16)	6.4 (13)	−0.9 (12)	3.8 (11)	−0.1 (12)
C(22)	−0.0821 (18)	−0.0647 (15)	0.2223 (7)	14.4 (18)	14.1 (21)	7.0 (10)	−0.5 (8)	6.6 (12)	2.1 (12)
C(23)	−0.1043 (19)	−0.0962 (12)	0.1339 (8)	14.2 (19)	7.5 (11)	12.2 (16)	−5.5 (14)	6.3 (12)	−0.3 (12)
C(24)	0.0409 (17)	−0.1438 (10)	0.1763 (7)	16.0 (21)	3.2 (10)	8.1 (13)	−0.4 (9)	1.9 (10)	3.5 (12)
C(25)	0.0686 (21)	0.2031 (14)	0.2039 (8)	17.4 (24)	9.2 (16)	6.6 (13)	−1.6 (12)	−1.3 (10)	−5.4 (14)
C(26)	0.1027 (17)	0.1698 (13)	0.2549 (7)	12.8 (20)	9.5 (15)	7.4 (13)	0.0 (10)	0.3 (10)	−4.0 (12)
C(27)	−0.0282 (18)	0.2303 (15)	0.2025 (10)	11.1 (17)	14.4 (16)	18.2 (19)	8.8 (16)	−3.9 (12)	−11.2 (16)
C(28)	0.1301 (18)	0.2602 (14)	0.1871 (9)	13.3 (21)	8.9 (15)	12.6 (16)	0.6 (7)	4.0 (12)	2.4 (14)
N(1)	0.4440 (9)	−0.1966 (7)	−0.0260 (6)	5.8 (7)	4.5 (6)	9.1 (10)	0.3 (6)	3.2 (6)	−1.1 (5)
C(29)	0.4729 (13)	−0.1500 (9)	0.0175 (6)	10.4 (14)	3.5 (10)	6.6 (10)	0.3 (9)	−1.0 (11)	−3.3 (8)
C(30)	0.5594 (14)	−0.1761 (11)	0.0431 (7)	8.6 (14)	6.4 (12)	10.1 (13)	2.3 (10)	−4.9 (11)	−2.6 (10)
C(31)	0.5829 (18)	−0.1157 (15)	0.0838 (9)	10.1 (17)	12.5 (20)	11.8 (16)	−0.1 (12)	−3.2 (12)	−1.0 (10)
C(32)	0.618 (3)	−0.056 (5)	0.0694 (21)	6.0 (29)	24.2 (62)	15.6 (44)	3.9 (38)	−2.5 (29)	−1.8 (49)
C(33)	0.3564 (12)	−0.1565 (10)	−0.0433 (7)	4.7 (10)	6.3 (11)	8.8 (13)	2.5 (9)	0.2 (10)	−1.8 (10)
C(34)	0.3126 (14)	−0.933 (11)	−0.0848 (8)	7.8 (15)	6.6 (12)	10.0 (16)	2.2 (11)	−1.7 (13)	−0.6 (12)
C(35)	0.2375 (18)	−0.1458 (13)	−0.1062 (7)	14.0 (20)	11.0 (17)	6.0 (13)	−0.1 (16)	−2.3 (13)	−1.3 (12)
C(36)	0.1871 (21)	−0.1684 (14)	−0.1488 (9)	17.1 (22)	9.0 (13)	11.5 (19)	−0.2 (14)	0.8 (16)	0.4 (14)
C(37)	0.5138 (12)	−0.2036 (10)	−0.0647 (7)	4.5 (11)	6.6 (12)	9.5 (13)	1.5 (9)	1.4 (10)	−0.7 (10)
C(38)	0.5410 (14)	−0.1316 (10)	−0.0861 (8)	8.3 (15)	4.9 (11)	11.9 (16)	0.7 (10)	3.0 (13)	1.0 (12)
C(39)	0.6015 (19)	−0.1494 (15)	−0.1285 (9)	13.6 (20)	11.3 (16)	12.1 (16)	−3.3 (15)	4.3 (14)	1.3 (14)
C(40)	0.6378 (25)	−0.0733 (18)	−0.1510 (9)	24.9 (30)	15.0 (24)	10.0 (16)	−3.0 (25)	7.1 (19)	0.9 (18)
C(41)	0.4216 (12)	−0.2808 (11)	−0.0106 (7)	4.8 (11)	10.3 (15)	8.0 (13)	1.8 (10)	2.8 (10)	0.1 (12)
C(42)	0.3490 (14)	−0.2862 (11)	0.0308 (8)	9.0 (15)	7.7 (13)	10.9 (16)	−0.7 (12)	1.9 (14)	−2.8 (14)
C(43)	0.3541 (25)	−0.3730 (14)	0.0537 (10)	23.3 (30)	8.4 (17)	12.9 (22)	0.6 (18)	11.9 (21)	0.1 (16)
C(44)	0.3117 (24)	−0.4185 (24)	0.0141 (16)	15.4 (29)	21.0 (34)	32.0 (40)	0[c]	0	0
N(2)	0.0087 (9)	0.1927 (8)	−0.0287 (6)	5.7 (11)	7.5 (10)	8.5 (10)	0.0 (8)	−1.9 (10)	3.4 (10)
C(45)	−0.0232 (13)	0.1457 (10)	0.0114 (6)	7.8 (14)	5.9 (11)	7.1 (13)	1.9 (10)	3.0 (10)	2.8 (10)
C(46)	−0.1125 (16)	0.1687 (11)	0.0360 (8)	11.9 (19)	6.3 (12)	10.3 (16)	1.9 (12)	−1.5 (14)	2.3 (12)
C(47)	−0.1355 (17)	0.1102 (15)	0.0733 (9)	10.3 (18)	13.5 (20)	11.0 (16)	1.6 (16)	1.2 (14)	5.2 (16)
C(48)	−0.2187 (24)	0.1300 (19)	0.1060 (12)	16.2 (29)	17.1 (29)	22.2 (31)	5.8 (23)	7.2 (24)	9.1 (20)
C(49)	0.0937 (13)	0.1550 (11)	−0.0463 (6)	6.0 (11)	7.9 (12)	6.3 (10)	1.7 (10)	2.1 (10)	2.5 (10)
C(50)	0.1469 (14)	0.1928 (13)	−0.0943 (8)	5.8 (12)	11.1 (17)	10.6 (16)	2.2 (12)	3.0 (11)	1.7 (14)
C(51)	0.2267 (22)	0.1405 (18)	−0.1067 (8)	18.1 (30)	16.7 (29)	10.1 (16)	−4.9 (22)	7.5 (24)	4.3 (15)
C(52)	0.269 (4)	0.1677 (26)	−0.1325 (19)	16.3 (29)	7.4 (12)	13.5 (17)	−5.0 (22)	0.6 (13)	3.6 (14)
C(53)	−0.0635 (15)	0.2024 (11)	−0.0709 (8)	9.6 (15)	5.7 (11)	10.6 (19)	1.1 (10)	−1.5 (14)	0.4 (12)
C(54)	−0.0917 (17)	0.1297 (14)	−0.0899 (9)	11.2 (17)	8.9 (17)	11.9 (16)	−0.7 (14)	−2.2 (14)	1.3 (14)
C(55)	−0.1474 (29)	0.1343 (18)	−0.1360 (14)	25.5 (37)	10.9 (22)	25.9 (40)	−0.8 (38)	−14.3 (29)	−4.8 (49)
C(56)	−0.1644 (25)	0.0748 (27)	−0.1638 (13)	15.4 (28)	24.8 (64)	21.5 (28)	0.4 (36)	−7.6 (26)	0.4 (22)
C(57)	0.0239 (14)	0.2778 (10)	−0.0126 (8)	7.9 (17)	5.4 (12)	13.0 (16)	0.2 (11)	−3.7 (13)	3.4 (12)
C(58)	0.0931 (16)	0.2851 (11)	0.0272 (10)	9.4 (16)	5.5 (11)	17.8 (22)	1.9 (11)	−2.5 (18)	−1.8 (16)
C(59)	0.073 (3)	0.3729 (18)	0.0647 (12)	32.8 (40)	9.8 (21)	20.1 (28)	−6.6 (25)	−12.9 (29)	4.9 (49)
C(60)	0.1263 (26)	0.3870 (25)	0.0268 (16)	16.9 (29)	22.8 (62)	29.7 (33)	7.5 (28)	−6.4 (25)	−4.2 (50)

[a] The form of the anisotropic thermal ellipsoid is $\exp[-0.25(B_{11}h^2a^{*2} + 2B_{22}k^2b^{*2} + b_{33}l^2c^{*2} + 2B_{12}hka^*b^* + 2B_{13}hla^*c^* + 2B_{23}klb^*c^*)]$. The quantities given in the table are in units of Å^2. [b] Disordered *tert*-butyl group. Methyl carbon atoms were refined with occupancy factors of 0.5. [c] End carbon atom of a cation *n*-butyl group. Full anisotropic refinement of this atom led to a negative thermal parameter.

Table III. Bond Distances (Å) and Selected Bond Angles (Deg) for the $Mo_2O_5(3,5\text{-}DBCat)_2^{2-}$ Anion

Inner Coordination Sphere			
Mo(1)-O(1)	1.915 (9)	Mo(2)-O(1)	1.923 (9)
Mo(1)-O(2)	1.700 (11)	Mo(2)-O(4)	1.674 (10)
Mo(1)-O(3)	1.707 (10)	Mo(2)-O(5)	1.701 (9)
Mo(1)-O(6)	2.164 (9)	Mo(2)-O(8)	2.148 (8)
Mo(1)-O(7)	1.978 (9)	Mo(2)-O(9)	1.975 (9)
Mo(1)-O(8)	2.371 (8)	Mo(2)-O(6)	2.399 (8)
O(2)-Mo(1)-O(3)	105.5 (5)	Mo(1)-O(1)-Mo(2)	109.4 (4)
O(2)-Mo(1)-O(1)	99.2 (4)	O(4)-Mo(2)-O(5)	104.3 (4)
O(2)-Mo(1)-O(7)	100.1 (5)	O(4)-Mo(2)-O(1)	99.4 (4)
O(2)-Mo(1)-O(6)	97.4 (4)	O(4)-Mo(2)-O(9)	99.9 (4)
O(2)-Mo(1)-O(8)	165.3 (4)	O(4)-Mo(2)-O(8)	98.7 (4)
O(3)-Mo(1)-O(1)	105.1 (4)	O(4)-Mo(2)-O(6)	166.3 (4)
O(3)-Mo(1)-O(7)	95.9 (4)	O(5)-Mo(2)-O(1)	107.3 (4)
O(3)-Mo(1)-O(6)	156.7 (4)	O(5)-Mo(2)-O(9)	94.3 (4)
O(3)-Mo(1)-O(8)	86.5 (4)	O(5)-Mo(2)-O(8)	156.3 (4)
O(1)-Mo(1)-O(7)	146.4 (4)	O(5)-Mo(2)-O(6)	86.8 (4)
O(1)-Mo(1)-O(6)	74.8 (3)	O(1)-Mo(2)-O(9)	146.3 (4)
O(1)-Mo(1)-O(8)	69.1 (3)	O(1)-Mo(2)-O(8)	74.1 (3)
O(7)-Mo(1)-O(6)	75.6 (4)	O(1)-Mo(2)-O(6)	69.2 (3)
O(7)-Mo(1)-O(8)	86.7 (3)	O(9)-Mo(2)-O(8)	75.9 (3)
O(6)-Mo(1)-O(8)	71.6 (3)	O(9)-Mo(2)-O(6)	86.9 (3)
Mo(1)-O(6)-Mo(2)	86.5 (3)	O(8)-Mo(2)-O(6)	71.3 (3)
		Mo(2)-O(8)-Mo(1)	87.6 (3)
Ligand I			
O(6)-C(1)	1.39 (2)	C(7)-C(3)	1.55 (3)
O(7)-C(2)	1.40 (2)	C(7)-C(8)	1.58 (2)
C(1)-C(2)	1.37 (2)	C(7)-C(9)	1.52 (3)
C(2)-C(3)	1.39 (2)	C(7)-C(10)	1.61 (3)
C(3)-C(4)	1.33 (3)	C(11)-C(5)	1.54 (3)
C(4)-C(5)	1.44 (3)	C(11)-C(12)	1.53 (4)
C(5)-C(6)	1.38 (2)	C(11)-C(13)	1.55 (6)
C(6)-C(1)	1.36 (2)	C(11)-C(14)	1.57 (5)
Mo(1)-O(6)-C(1)	114.7 (8)	O(6)-C(1)-C(6)	123.2 (14)
Mo(1)-O(7)-C(2)	119.2 (8)	O(7)-C(2)-C(3)	121.9 (13)
O(6)-C(1)-C(2)	113.5 (13)	Mo(2)-O(8)-C(15)	134.5 (7)
O(7)-C(2)-C(1)	116.4 (13)		
Ligand II			
O(8)-C(15)	1.33 (2)	C(21)-C(17)	1.15 (3)
O(9)-C(16)	1.36 (2)	C(21)-C(22)	1.63 (3)
C(15)-C(16)	1.37 (2)	C(21)-C(23)	1.57 (3)
C(16)-C(17)	1.35 (2)	C(21)-C(24)	1.57 (3)
C(17)-C(18)	1.45 (2)	C(25)-C(19)	1.66 (3)
C(18)-C(19)	1.38 (2)	C(25)-C(26)	1.63 (3)
C(19)-C(20)	1.36 (2)	C(25)-C(27)	1.46 (4)
C(20)-C(15)	1.42 (2)	C(25)-C(28)	1.42 (4)
Mo(2)-O(8)-C(15)	133.2 (8)	O(8)-C(15)-C(20)	121.9 (13)
Mo(2)-O(9)-C(16)	118.8 (8)	O(9)-C(16)-C(17)	122.8 (13)
O(8)-C(15)-C(16)	116.5 (13)	Mo(2)-O(6)-C(1)	137.2 (7)
O(9)-C(16)-C(15)	115.0 (13)		

trolysis experiment: high concentration of electrocycle, coordinating solvent (DMF). Our conclusion from this experiment is that the $Mo_2O_5(3,5\text{-}DBCat)(3,5\text{-}DBSQ)^-$ complex has a localized electronic structure on the EPR time scale at room temperature and does not show interligand electron transfer.

Oxygen-Transfer Reactions of Molybdenum-Catechol Complexes

Oxygen atom transfer reactions involving molybdenum are related to a fundamental biological function of the metal and have been of considerable general interest. Factors that destabilize terminal oxo ligands are related to d configuration, d orbital population decreases π donation, and competitive bonding by other strong π-donor ligands. Complexes obtained from the $Mo(CO)_6$–quinone reactions (1) are related by the substitution of oxo oxygen atoms by unreduced *o*-benzoquinones as shown in Scheme I. To date no single quinone ligand has been found to form more than two members of this series; $Mo_2O_5(9,10\text{-}phenSQ)_2$ can be converted to $Mo(phenCat)_3$.[20] Rational procedures are being developed to interconvert members of this cycle, and it appears that the unusual stability of the oxygen-deficient members of this series [$Mo^{VI}(Cat)_3$, $Mo^{VI}O(Cat)_2$] toward addition of larger numbers of oxo ligands is related to the strong π-donor bonding of the catecholate ligands.[21]

Table IV. Dihedral Angles and Least-Squares Planes for the $Mo_2O_5(3,5\text{-}DBCat)_2^{2-}$ Anion

Least-Squares Planes

atom	dist, Å	atom	dist, Å
Ligand I			
$12.56x - 4.84y - 10.97z = 3.18$			
Mo(1)	0.253	C(4)	−0.009 (17)
O(6)	0.030 (8)	C(5)	−0.055 (17)
O(7)	−0.013 (10)	C(6)	−0.072 (17)
C(1)	−0.032 (13)	C(7)	0.082 (22)
C(2)	−0.050 (16)	C(11)	0.121 (22)
C(3)	0.030 (17)		
Ligand II			
$11.92x - 5.45y + 12.84z = 2.40$			
Mo(2)	−0.179	C(18)	−0.009 (18)
O(8)	−0.040 (8)	C(19)	0.022 (17)
O(9)	0.033 (9)	C(20)	0.053 (15)
C(15)	0.055 (13)	C(21)	−0.122 (21)
C(16)	0.024 (15)	C(25)	−0.070 (28)
C(17)	−0.013 (16)		

Dihedral Angles

plane 1	plane 2	angles, deg
ligand I	ligand II	50.0 (4)
O(4)-O(5)-O(9)	O(2)-O(3)-O(7)	6.9 (4)
O(4)-O(5)-O(9)	O(1)-O(6)-O(8)	7.1 (4)
O(2)-O(3)-O(7)	O(1)-O(6)-O(8)	6.1 (4)
Mo(1)-O(6)-O(8)	Mo(2)-O(8)-O(6)	115.8 (4)

Scheme II

$$[MoO(3,5\text{-}DBCat)_2]_2 + 2OH^- \rightarrow 2MoO(OH)(3,5\text{-}DBCat)_2^-$$

$$MoO(OH)(3,5\text{-}DBCat)_2^- + 2OH^- \rightarrow MoO_2(OH)(3,5\text{-}DBCat)^- + 3,5\text{-}DBCat^{2-} + H_2O$$

$$2MoO_2(OH)(3,5\text{-}DBCat)^- \rightarrow Mo_2O_5(3,5\text{-}DBCat)_2^{2-} + H_2O$$

net reaction:

$$[MoO(3,5\text{-}DBCat)_2]_2 + 6OH^- \rightarrow Mo_2O_5(3,5\text{-}DBCat)_2^{2-} + 2(3,5\text{-}DBCat^{2-}) + 3H_2O$$

The procedure used to synthesize $Mo_2O_5(3,5\text{-}DBCat)_2^{2-}$ involved the addition of strong base to $[MoO(3,5\text{-}DBCat)_2]_2$ in a three-step process, which has been reported to be catalyzed by molecular oxygen.[11] The first step shown in Scheme II involves dissociation of the dimer to form the six-coordinate *trans*-$MoO(OH)(3,5\text{-}DBCat)_2^-$ complex anion. This reaction is similar to the six-coordinate solvates $MoO(Sol)(3,5\text{-}DBCat)_2$ formed by the dimer in coordinating solvents. What is of particular interest is that addition of acid to a black solution of $K[MoO(OH)(3,5\text{-}DBCat)_2]$ formed by treating the dimer with ethanolic KOH leads to re-formation of the purple dimer, which can be extracted with toluene. Therefore OH^- addition in the first step of this scheme seems to be reversible.

What is discouraging about this chemistry is the apparent instability of the neutral $Mo_2O_5(3,5\text{-}DBSQ)_2$ complex. This may indicate that the specific bonding properties of the individual quinone ligands are important in stabilizing members of the series shown in Scheme I and that no single ligand can be used to form complexes of all three types.

---

(20) Pierpont, C. G.; Buchanan, R. M. *J. Am. Chem. Soc.* **1975**, *97*, 4912.

(21) Shorthill, W. B.; Buchanan, R. M.; Pierpont, C. G.; Ghedini, M.; Dolcetti, G. *Inorg. Chem.* **1980**, *19*, 1803.

Acknowledgment. We wish to thank the National Institutes of Health for support of this research under Grant GM-23386 and the National Science Foundation for support to purchase the EPR instrumentation.

Registry No. (n-$Bu_4N)_2[Mo_2O_5(3,5\text{-DBCat})_2]$, 74521-90-7.

Supplementary Material Available: Listing of structure factor amplitudes (11 pages). Ordering information is given on any current masthead page.

Contribution from the Departments of Chemistry, University of Nebraska, Lincoln, Nebraska 68588, and University of California, Berkeley, California 94720

Modes of Phosphite Reactions with Transition-Metal Complexes. Crystal Structures of $(\eta^5\text{-}C_5H_5)Cr[P(O)(OCH_3)_2](CO)_2[P(OCH_3)_3]$ and $\{(CH_3O)_2PMo[P(OCH_3)_3]_5{}^+\}(PF_6{}^-)$

V. W. DAY,*[1a] I. TAVANAIEPOUR,[1a] S. S. ABDEL-MEGUID,[1a] J. F. KIRNER,[1b] L.-Y. GOH,[1c] and E. L. MUETTERTIES*[1b]

Received June 4, 1981

Trialkyl phosphites typically interact with transition-metal ions or complexes to form phosphite–metal donor–acceptor bonds. Aberrant forms of interactions include P–O and R–O (ROP) cleavage reactions. Crystal structures of two complexes that are the end result of P–O and R–O (ROP) bond cleavage reactions between metal complexes and trimethyl phosphite are described. The complexes are $(\eta^5\text{-}C_5H_5)Cr[P(O)(OCH_3)_2](CO)_2[P(OCH_3)_3]$ (**1**) and $\{(CH_3O)_2PMo[P(OCH_3)_3]_5{}^+\}(PF_6{}^-)$ (**2**), respectively. Crystals of **1** were monoclinic with space group $P2_1/n$ (a = 7.853 (1) Å, b = 29.761 (5) Å, c = 15.203 (2) Å, β = 105.02 (1)°, Z = 8, V = 3432 Å^3). The asymmetric unit of the crystal contained two crystallographically independent molecules, which differed essentially only in the sense of the orientation of the methyl groups of the trimethyl phosphite ligand. Square pyramidal is a simple and accurate description of the observed chromium coordination sphere with the unique apical ligand represented by the C_5 centroid–Cr vector; here the C_5H_5–Cr interaction formally is considered as a single coordination site. There is a significantly longer Cr–P distance for the phosphonate ligand than for the neutral phosphite ligand. Crystals of **2** were triclinic with space group $P\bar{1}$-C_i^1 (a = 10.336 (2) Å, b = 12.700 (2) Å, c = 15.518 (3) Å, α = 92.72 (1)°, β = 105.52 (1)°, γ = 87.86 (1)°, Z = 2, V = 1960 Å^3) and contained $\{(CH_3O)_2PMo[P(OCH_3)_3]_5{}^+\}$ and $PF_6{}^-$ ions. An octahedral array of phosphorus ligands prevailed in the molybdenum cationic complex. Close packing of CH_3O groups on the periphery of the complex gave close CH_3–O···P interligand contacts, and this feature may be responsible for the facile exchange of CH_3O groups between inequivalent phosphorus atoms.

Introduction

Formation of metal–phosphorus donor–acceptor bonds with organophosphines and phosphites can lead to subsequent reaction sequences in which C–H bonds are cleaved to finally generate structures of types **3**–**5**. Such C–H bond scission

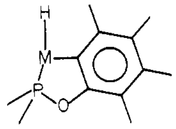

3

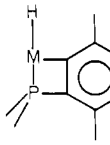

4

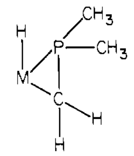

5

is most facile for aryl phosphites,[2-4] **3**, followed by arylphosphines,[2-4] **4**, and then alkylphosphines,[2-4] **5**—especially for those intermediates that are coordinately unsaturated. For a period of time, we had thought that trialkyl phosphites were relatively immune to subsequent reactivity problems except at high temperatures but it is clear from literature reports and from our own research that reactivity problems do arise and the reaction sequences are qualitatively distinct. For example, we have found that $(CH_3O)_3P$ reacts with $Ir_4(CO)_{12}$ at elevated temperatures through a catalytic Arbuzov rearrangement to yield $CH_3P(O)(OCH_3)_2$.[5] Also, it has been shown[6] that thermolysis of metal trimethyl phosphite complexes can generate polyfunctional phosphite ligands: $Os_3(CO)_{11}P(OCH_3)_3$ yields a complex, $HOs_5C(CO)_{12}[OP(OCH_3)OP(OCH_3)_2]$, with the trifunctional ligand O–$P(OCH_3)$–O–$P(OCH_3)_2$.

Methyl group migration is a relatively common reaction of coordinated trimethyl phosphite. For example, a simple and clean illustration is the transformation of $Ru[P(OCH_3)_3]_5$ to $CH_3Ru[P(O)(OCH_3)_2][P(OCH_3)_3]_4$ at temperatures above 150 °C.[7] An analogous, but much more facile, methyl group transfer takes place in the reaction of $\{\eta^5\text{-}C_5H_5Cr(CO)_2P(OCH_3)_3\}_2$ with trimethyl phosphite to give $(\eta^5\text{-}C_5H_5)Cr(CH_3)(CO)_2P(OCH_3)_3$ and the phosphonate complex $(\eta^5\text{-}C_5H_5)Cr[P(O)(OCH_3)_2](CO)_2P(OCH_3)_3$ (**1**).[8] Similar molybdenum chemistry has been reported earlier.[9] Another example of phosphite methyl group transfer is the conversion of $\{(C_5H_5)(CH_3)Rh[P(OCH_3)_3]_2{}^+\}I^-$ to $(C_5H_5)(CH_3)Rh[P(O)(OCH_3)_2]P(OCH_3)_3$ and CH_3I.[10] Phosphite addition[11] on the π-arene ligand, not the metal atom, in $(C_6H_6)_2M^{2+}$ (M = Fe, Ru) yields the phosphonium complex $\{\eta^6\text{-}C_6H_6M[\eta^5\text{-}C_6H_6P(OCH_3)_3]^{2+}\}$, which can be converted to the phosphonate, $\{(\eta^6\text{-}C_6H_6)M[(\eta^5\text{-}C_6H_6)P(O)(OCH_3)_2]^+\}$, by $CH_3{}^+$ loss. Another surprising aspect of coordinated trimethyl phosphite chemistry is the rapid cleavage of the P–O bond on protonation of $M[P(OCH_3)_3]_6$, M = Mo[12] or W,[13] by trifluoroacetic acid to give $\{(CH_3O)_2PM[P(OCH_3)_3]_5{}^+\}$ rather than the selective formation of $\{HM[P(OCH_3)_3]_6{}^+\}$. Single crystals of the molybdenum salt $\{(CH_3O)_2PMo[P(OCH_3)_3]_5{}^+\}(PF_6{}^-)$ (**2**) were

---

(1) (a) University of Nebraska. (b) University of California. (c) On leave from the Department of Chemistry, University of Malaya, Kuala Lumpur, Malaysia.

(2) For discussions of this type of behavior in coordinated phosphines, see ref 3 and 4.

(3) Parshall, G. W. *Acc. Chem. Res.* **1970,** *3,* 139; **1975,** *8,* 113.

(4) Harris, T. V.; Rathke, J. W.; Muetterties, E. L. *J. Am. Chem. Soc.* **1978,** *100,* 6966.

(5) Schunn, R. A.; Demitras, G. C.; Choi, H. W.; Muetterties, E. L. *Inorg. Chem.* **1981,** *20,* 4023.

(6) Orpen, A. G.; Sheldrick, G. M. *Acta Crystallogr., Sect. B* **1978,** *B34,* 1992.

(7) Pomeroy, R. K.; Alex, R. F. *J. Chem. Soc., Chem. Commun.* **1980,** 1114.

(8) Goh, L.-Y.; D'Aniello, M. J., Jr.; Slater, S.; Muetterties, E. L.; Tavanaiepour, I.; Chang, M. I.; Fredrich, M. F.; Day, V. W. *Inorg. Chem.* **1979,** *18,* 192.

(9) Haines, R. J.; Nolte, C. R. *J. Organomet. Chem.* **1970,** *24,* 725.

(10) Werner, H.; Feser, R. *Z. Anorg. Allg. Chem.* **1979,** *458,* 301.

(11) Sweigart, D. A. *J. Chem. Soc., Chem. Commun.* **1980,** 1159.

(12) Muetterties, E. L.; Kirner, J. F.; Evans, W. J.; Watson, P. L.; Abdel-Meguid, S. S.; Tavanaiepour, I.; Day, V. W. *Proc. Natl. Acad. Sci. U.S.A.* **1978,** *75,* 1056.

(13) Choi, H. W.; Gavin, R. M.; Muetterties, E. L. *J. Chem. Soc., Chem. Commun.* **1979,** 1085.

0020-1669/82/1321-0657$01.25/0